

DR. ALBERTO MONJE (Orcid ID : 0000-0001-8292-1927)

DR. SIGRUN EICK (Orcid ID : 0000-0002-4619-2461)

Article type : Original Article

## **Microbial and host-derived biomarker changes during ligature-induced and spontaneous peri-implantitis in the Beagle dog**

Alberto Monje, DDS, MS, PhD, \*† Sigrun Eick, PhD, \*\* Daniel Buser, DDS, MS, PhD<sup>¶</sup>  
Giovanni E. Salvi, DDS

\* Department of Periodontology, Universidad Internacional de Catalunya, Barcelona, Spain

† Department of Periodontology, School of Dental Medicine, University of Michigan, Ann Arbor, USA

\*\* Department of Periodontology, University of Bern, Bern, Switzerland

<sup>¶</sup> Department of Stomatology and Oral Surgery, University of Bern, Bern, Switzerland

### **Corresponding author:**

Alberto Monje, DDS, MS, PhD

Department of Periodontology Universitat Internacional de Catalunya

C/ Josep Trueta s/n, 08195

Sant Cugat del Vallès. Barcelona. Spain. Tel: 0034 93 504 20 00

E-mail address: amonjec@umich.edu

Telephone: +34924203045

**Word account:** 2423

**Running title:** Microbiota and host-related factors in peri-implantitis

This is the author manuscript accepted for publication and has undergone full peer review but has not been through the copyediting, typesetting, pagination and proofreading process, which may lead to differences between this version and the [Version of Record](#). Please cite this article as [doi: 10.1111/JRE.12797](https://doi.org/10.1111/JRE.12797)

This article is protected by copyright. All rights reserved

**One sentence summary:** Experimental peri-implantitis is led by an increase of unspecific bacteria.

**Conflict of interest:** The authors declare no direct conflict of interest. Dr. A. Monje received honoraria from TICARE Implants (Valladolid, Spain) and research funding.

**Abstract:**

1. *Objective:* To evaluate microbial and host-derived biomarker changes during experimental peri-implantitis in the Beagle dog.
2. *Background:* Limited data exists on the microbial and biomarker changes during progressive bone loss as result of experimental peri-implantitis.
3. *Methods:* In total, 36 implants ( $n_{\text{dogs}}=6$ ) were assessed over 3 episodes of ligature-induced peri-implantitis followed by a period of spontaneous progression. Implants with hybrid (H) and completely rough (R) surface designs were used. Clinical and radiographic parameters were recorded at 4 timepoints. Peri-implant sulcus fluid was collected from the buccal and lingual aspects of the implants. The presence of 7 bacterial species and 2 host-derived biomarkers was assessed during the study period.
4. *Results:* Total bacterial counts were significantly correlated with marginal bone loss (MBL) ( $r=0.21$ ;  $p=0.009$ ). Further, *Phorphyromonas gulae* (*Pg*) and *Tannerella forsythia* (*Tf*) were commonly correlated with MBL, suppuration (SUP) and the sulcular bleeding index scores (mSBI) ( $p<0.05$ ). Other bacteria were further correlated with SUP, mSBI and MBL. While the analyzed bacteria dropped, *Prevotella intermedia* (*Pi*) further increased during the spontaneous progressive phase ( $p<0.05$ ). Total bacterial load did not differ significantly between H and R implants. Host-derived IL-10 was undetected along the study period. IL-1 $\beta$  positively correlated with probing pocket depth ( $r=0.18$ ;  $p=0.03$ ). During spontaneous progression, H implants displayed statistically significant lower levels of IL-1 $\beta$  ( $p=0.003$ ).
5. *Conclusion:* Experimental peri-implantitis is associated with an increase in bacterial counts. While *Pg* and *Tf* are associated with ligature-induced disease progression, *Pi* augmented its load during the spontaneous progressive phase. IL-1 $\beta$  is associated with pocket probing depth and influenced by implant surface characteristics during the spontaneous progression phase.

## **Introduction**

Peri-implantitis is conceived as a biofilm-mediated inflammatory condition characterized by progressive loss of the supporting tissues. In fact, outcomes from preclinical and clinical human studies demonstrated that the deposition of plaque on dental implants induce peri-implant mucositis and peri-implantitis. It has been further documented that disease onset and progression are associated with qualitative and quantitative differences in the microbiome when compared with peri-implant health.<sup>1</sup> In point of fact, it was demonstrated that within an hour after implant surgery, bacteria colonize the peri-implant environment and a complex biofilm is formed within 2 weeks.<sup>2</sup> Data from reports indicate that peri-implantitis is a heterogeneous mixed infection including periodontopathic organisms, uncultivable anaerobic gram+ and gram- rods, enteric rods and *Staphylococcus aureus*.<sup>3-5</sup>

Biopsies from human peri-implantitis lesions display inflammatory infiltrates more than twice as large as those noted at periodontitis sites.<sup>6</sup> In addition, it is featured by larger numbers and densities of plasma cells, macrophages, neutrophils, and a higher density of vascular structures outside and lateral to the cell infiltrate compared to periodontitis sites.<sup>6</sup> Hence, in spite of the conflicting data that has evidenced the morphological and immunophenotypical differences between peri-implantitis and periodontitis, the former has shown to be more severe in inflammatory infiltrate.<sup>7</sup> In this sense, peri-implantitis has demonstrated an increase in bone turnover markers, proinflammatory cytokines, such as tumor necrosis factor or interleukin-1, and proteinases, considered as valid and accurate molecules to monitor peri-implant disorders.<sup>8-10</sup>

Therefore, the purpose of the present preclinical *in vivo* study was to assess the colonization and shifts in microbiota and host-derived biomarkers in the course of ligature-induced and spontaneous progression of peri-implantitis in dogs.

## **Material and methods**

The study protocol was submitted and approved by the Local Ethics Committee (Government of Extremadura, Health and Social Policy Council, Extremadura, Spain [#2017209030001787]) in compliance with the pertinent local and European regulations (REGA ES 100370001499). Furthermore, the study followed the ARRIVE (Animal Research: Reporting of *In Vivo* Experiments) guidelines developed as part of an NC3Rs initiative to improve the design, analysis and reporting of studies involving animals.<sup>11</sup>

### *Experimental design*

An *in vivo* animal study involving six healthy Beagle dogs<sup>12</sup> of approximately 1 year were used for this study. The animals were housed under laboratory conditions. The recommended humidity for the room is >30%. The light cycle was controlled using an automatic timer (12 hours light, 12 hours dark). The animals were fed a daily pellet diet. All the specimens presented intact maxillary arches, without any general occlusal trauma or oral viral or fungal lesions.

### *Tooth extraction and implant installation*

Mandibular premolar and molar extractions (P2 – M1) were performed in the hemi-arches of each dog. On the buccal as well as on the lingual aspect of the ridge, minimal

full-thickness flaps were elevated to disclose the marginal portion of the periodontal tissues. The teeth were sectioned in a bucco-lingual direction at the bifurcation using a tungsten carbide burr so that the roots could be individually extracted using a periotome and forceps, without damaging the bony walls. The wound margins were stabilized with a continuous interlocking suture.

Implant placement was performed 8 weeks after dental extraction. Following crestal incision and flattening of the edentulous ridge with a round bur, implants were placed following manufacturer's instructions. Two different implants based on their coronal design were tested: rough up to the platform (R) (TiCare Inhex Mini 3.3 × 8 mm; roughness: 1.2-1.6 Ra - Mozo-Grau, Valladolid, Spain) and hybrid (H) (TiCare Inhex Mini 3.3 × 8 mm; roughness of machined surface: 0.2 Ra/roughness of moderately rough surface: 1.2-1.6 Ra - Mozo-Grau, Valladolid, Spain) with 1.5 mm of machined surface at the coronal aspect (Figure 1). Both implant designs were platform-switch design. The micro-rough surface for R and H implants was hydrophobic resorbable blast media (RBM-TC). Altogether, 6 implants were randomly inserted per animal (3 by side). All study implants healed under a submerged environment and received a one-piece healing abutment at 8 weeks. The flaps were re-adapted around the healing abutments with interrupted sutures to preserve at least 2mm of keratinized mucosa around the implants to anticipate peri-implant tissue health.<sup>13</sup> Oral hygiene was performed daily, consisting of daily brushing with pumice combined with 0.12% chlorhexidine digluconate followed by topical application of 0.12% chlorhexidine digluconate spray for a total of 3 weeks.

#### *Ligature-induced peri-implantitis*

The detailed ligature-induced peri-implantitis protocol can be found elsewhere.<sup>12</sup> Briefly, after 8 weeks of healing, silk ligatures (3/0) were placed looping the apical portion of the implant-supported healing abutments and changed three weeks apart for a total of three events (T1: 3 weeks; T2: 6 weeks; T3: 9 weeks). All ligatures were removed after three weeks with sustained deprivation of oral hygiene to test the spontaneous progression of peri-implantitis (T4: 12 weeks).

#### *Clinical analysis*

As published elsewhere,<sup>12</sup> the clinical assessment was carried out with a North Carolina probe (Hu-Friedy, Chicago, IL, USA) using controlled force probe about 17g to evaluate four different clinical parameters: pocket probing depth (PPD), sulcular bleeding on probing (mSBI)<sup>14</sup>, mucosal recession (MR) and suppuration (SUP)

#### Radiographic analysis

As published elsewhere,<sup>15</sup> all images were obtained using computed tomography (CT) (Phillips Medical System, The Netherlands) under general anesthesia following each clinical examination. The imaging parameters were set at 120 kV, with an increment of 0.5 mm, a slice thickness of 1 mm, a mAs/slice ratio of 250, collimation 6x0.75 and a matrix of 512, with a field of view (FOV) sufficient to scan the mandibular body. Data were saved in the Digital Imaging and Communications in Medicine (DICOM) format and reconstructed to obtain cross-sectional slides (Osirix MD, Bernex, Switzerland) using a desktop computer. Distance from the implant platform to the first coronal bone-to-implant contact was determined in four positions per implant: mesio-buccal (MB), mesio-lingual (ML), disto-lingual (DL) and disto-buccal (DB). These measurements were carried four times (at each timepoint: T1, T2, T3 and T4).

#### *Sampling of peri-implant sulcus fluid and microbial/host-derived markers analyses*

Peri-implant sulcus fluid was collected at the buccal and lingual aspects of each site by means of sterile paper strips (Periopaper; Oraflow Inc., Smithtown, NY, USA) at 3 timepoints during the ligature-induction of peri-implantitis (T1-T3) and at T4 during spontaneous progression of peri-implantitis. Paper strips were placed at the entrance of the crevice and left in place for 30 s. Subsequently, the paper stripes were transferred to tubes placed in ice and stored at -80°C until analysis. Samples were eluted at 4°C overnight into 600 µl phosphate-buffered saline containing proteinase inhibitors (Sigma-Aldrich, St. Louis, MO, USA). From the eluates, the levels of interleukin IL-1β and IL-10, were determined by using commercially available enzyme-linked immunosorbent assay (ELISA) kits according to manufacturer's instructions. Furthermore, DNA was extracted using the Chelex method for real-time PCR and performed for the bacterial species *Neisseria canis* (Nc), *Prevotella intermedia* (Pi), *Fusobacterium nucleatum* (Fn), *Porphyromonas gulae* (Pg), *Tannerella forsythia* (Tf), *Campylobacter rectus* (Cr) and *Parvimonas micra* (Pm) known to be involved in periodontal biofilm formation in dogs.<sup>16, 17</sup> Total bacterial counts were also tested (16S).

### Statistical analysis

To test correlations at implant and site levels, Pearson's lineal correlation coefficient was applied. Lineal regression equations (GEE) were calculated from microbiological and host-related markers analyses. Same calculations were applied to test the effect of implant design on the microbiological and host-derived markers features. Chi<sup>2</sup> Wald was applied to provide the 95% confidence intervals (CI) for the 4 timepoints evaluated. The level of statistical significance was set at 0.05.

### Results

Overall, 36 implants were followed up during 3 episodes of ligature-induced peri-implantitis (T1-T3) and 1 stage of spontaneous progression (T4). No implant loss occurred along the study period. Mean MBL at T4 was 5±0.7mm (Figure 2). Mean clinical values/scores along the study period for the clinical and radiographic parameters can be found elsewhere.<sup>12</sup>

### Microbial profile during experimental peri-implantitis

Total bacterial counts (16S) and all the analyzed bacteria significantly increased their load during induction (compared to T1 -  $p < 0.001$ ) and slightly dropped during the stage of spontaneous progression with the exception of *Pi*, which significantly raised further from T3 to T4 ( $p < 0.05$ ) (Figure 3). Total bacterial count was significantly correlated with MBL ( $r = 0.22$ ;  $p = 0.009$ ) (Figure 4a). Alike, *Pg* ( $r = 0.36$ ;  $p < 0.001$ ), *Tf* ( $r = 0.23$ ;  $p = 0.006$ ), *Fn* ( $r = 0.36$ ;  $p < 0.001$ ) and *Cr* ( $r = 0.25$ ;  $p = 0.003$ ) were further correlated with MBL. No significant associations were identified for PPD or MR and microbiota. Nevertheless, 16S ( $r = 0.20$ ;  $p = 0.01$ ), *Pg* ( $r = 0.31$ ,  $p < 0.001$ ), *Tf* ( $r = 0.16$ ;  $p = 0.04$ ) and *Fn* ( $r = 0.24$ ;  $p = 0.004$ ) reached statistically significant correlations with mSBI (Figure 4b). Along these lines, SUP exhibited significance with *Pg* ( $r = 0.22$ ;  $p = 0.009$ ), *Tf* ( $r = 0.22$ ;  $p = 0.007$ ), *Nc* ( $r = 0.24$ ;  $p = 0.003$ ) and *Cr* ( $r = 0.19$ ;  $p = 0.02$ ) (Supplementary table 1). When comparing specific implant sites, 16S ( $r = 0.24$ ;  $p = 0.004$ ), *Pg* ( $r = 0.32$ ;  $p = 0.001$ ), *Tf* ( $r = 0.24$ ;  $p = 0.004$ ), *Fn* ( $r = 0.35$ ;  $p < 0.001$ ), and *Cr* ( $r = 0.27$ ;  $p < 0.001$ ) were significantly correlated with MBL at buccal sites, while *Pg* ( $r = 0.30$ ;  $p < 0.001$ ), *Fn* ( $r = 0.28$ ;  $p = 0.001$ ) and *Cr* ( $r = 0.18$ ;  $p = 0.03$ ) were significantly correlated with MBL at lingual sites.

### Significance of implant design on microbial profile

Total bacterial load did not differ significantly between H and R implants along the study period. Total bacterial counts at T4 were 7.06 and 7.11 for H and R implants. R implants exhibited a mean of 0.07 units less of total bacterial counts along the study period. Interestingly, R implants displayed statistically significantly lower bacterial counts for *Tf* ( $p=0.01$ ) - in particular at T1 ( $p=0.03$ ) and T2 ( $p=0.001$ ) and *Fn* ( $p=0.01$ ) - in particular at T3 ( $p<0.001$ ). On the other side, *Pi* exhibited statistically significant lower values for H implants along the study period ( $p=0.04$ ) - in particular with strong statistical significance at T3 ( $p<0.001$ ) (Supplementary table 2)

### **Host-derived markers during experimental peri-implantitis**

The anti-inflammatory cytokine IL-10 was not identified along the study period. For the pro-inflammatory cytokine IL-1 $\beta$ , a statistically significant increase was found along the study period. In fact, a non-statistically significant tendency towards significance was demonstrated when correlated with MBL ( $r=0.13$ ;  $p=0.13$ ). A statistical moderate significant correlation was reached with PPD ( $r=0.18$ ;  $p=0.03$ ) (Figure 4c).

### **Significance of implant design on host-derived markers**

Despite no statistically significant differences could be attributed to implant design along the study period, a significant drop of  $\sim\frac{1}{2}$  of the mean value in IL-1 $\beta$  was noted for H implants during spontaneous progression of peri-implantitis while at R implants a statistically significant increase of  $\sim 2x$  in the mean value at T4 ( $p=0.003$ ) was observed (Figure 5).

## **Discussion**

### ***Main findings***

This preclinical experimental peri-implantitis study shed light on the microbial and host-derived markers in the course of the disease as follows: (1) peri-implantitis progression induced by ligature is associated with an increase in periodontopathic bacteria, (2) putative pathogens such as *Pg* and *Tf* are commonly associated with progressive bone loss and the presence and profuseness of mSBI and SUP, (3) spontaneous progression of peri-implantitis is characterized by a decrease in pathogenic bacterial counts (except *Pi* that further increased) along with the reduction in clinical parameters and, (4) implant surface might play a role upon the spontaneous progression of experimental peri-implantitis in terms of IL-1 $\beta$ .



### ***Are our findings consistent with previous results?***

A limited number of experimental studies elucidated the distinct bacterial and host-derived features in the course of peri-implantitis. Eke et al. (1998) assessed at 5 time-points the microbiota associated with experimental peri-implantitis in adult *Macaca mulatta* monkeys. It was shown the role of *spirochetes* in disease progression as they were correlated with increase in PPD and MBL. Furthermore, levels of *Pi* were positively correlated with BOP while levels of *Actinomyces actinomycetecomitans* were negatively correlated with BOP.<sup>18</sup> Tillmanns et al. (1998) demonstrated in beagle dogs that *Actinomyces actinomycetecomitans*, *Pi* and *Pg* were consistent across the samples at the end of the experimental peri-implantitis study period.<sup>19</sup> Later on, Junior et al. (2000) evaluated the attachment loss and bacterial profile in experimental peri-implantitis in mongrel dogs. Interestingly, *Tf* and *Pg* presented strong association with MBL, while other putative bacteria such as *Actinomyces actinomycetecomitans*, *Pi* and *Prevotella nigrescens* were undetected along the study period.<sup>20</sup> More recently, it was evidenced that *Pg* and *Tf* increased significantly along the ligature-induced peri-implantitis experimental phase.<sup>21</sup> Our findings, therefore, are consistent with previous results on the increase in bacterial counts, in particular *Pg* and *Tf*, during ligature-induced peri-implantitis. On the other hand, Charalampakis et al. (2014) showed in beagle dogs that the total bacterial load increased during the period following ligature removal and established an anaerobic Gram-negative microflora.<sup>1</sup> The later findings can be attributed to the longer phase of spontaneous progression compared to ours. Nevertheless, observations from the present study partially agreed with Charalampakis et al. as the *Pi* counts significantly increased from T3 (0.21) to T4 (0.34).

The results of the present experimental study suggested that bacteria such as *Pg*, *Tf*, *Fn* and *Cr* are significantly associated with progressive bone loss. Interestingly, *Pg* and *Tf*, were further significantly associated with mSBI and SUP. Hence, based on the fact that *Pg* and *Tf* proved to be associated with radiographic and clinical signs of disease progression underlined the concept that this nonmotile anaerobic Gram - bacteria seems relevant in the progression of the disease. Therefore, findings from the present study supported the feasibility of microbial analysis to monitor disease progression. Furthermore, in light of these findings, it could be speculated that the use of antibiotics to target nonmotile anaerobic Gram - bacteria might be beneficial for the resolution of

peri-implantitis, as also suggested by clinical studies on the management of peri-implantitis.<sup>22-24</sup>

This experimental study could not identify IL-10 along the study period whereas IL-1 $\beta$  displayed a tendency towards statistical significance with peri-implantitis progression. These findings are contemplated within the context that peri-implantitis lesions display a significant increase in the population of M1 macrophages compared to periodontitis, which express high level of pro-inflammatory mediators in contrast to M2 macrophages that are associated with the production of IL-10.<sup>25</sup> In addition, to our knowledge this interleukin has not been experimentally tested in preclinical studies on peri-implantitis. Nevertheless, outcomes from human studies indicated increased levels of this pro-inflammatory cytokine in patients with peri-implantitis.<sup>9, 26, 27</sup> For instance, Renvert et al. (2015) evidenced that profuse bleeding and/or SUP was associated with higher levels of IL-1 $\beta$ .<sup>26</sup> The present study indicated that IL-1 $\beta$  is significantly correlated with PPD. This finding is not surprising since this cytokine is produced by activated macrophages and is an important mediator of the inflammatory response, and is involved in a wide array of cellular activities such as cell proliferation or apoptosis.<sup>28</sup> Interestingly, these findings did not find a correlation between IL-1 $\beta$  and SUP or mSBI. This might be attributable to the inherent shortcomings associated with this experimental model and the short-term duration of the study. More robust findings concerning the pro-inflammatory profile would benefit from the analysis of multiple proinflammatory cytokines such as IL-6 or tumor necrosis factor (TNF).

### ***Limitations***

The present study has drawbacks that must be disclosed. First, scarce evidence indicates that ligature-induced model resembles naturally occurring peri-implantitis.<sup>29</sup> Episodes of experimental induction were applied every 3-weeks. This is a relative short time frame compared to other investigations on the same matter.<sup>1, 30, 31</sup> In addition, only 7 bacteria were tested, while the core peri-implantitis microbiome is known to be significantly wider based on previous experimental reports and human findings on naturally occurring peri-implantitis.<sup>1, 4, 32</sup>

Moreover, it is worth to note that that bone measurements were carried out using CT instead of intraoral radiographs (IR). In fact, CT may overcome limitations inherent to

IR such as superimpositioning<sup>33</sup> or the impaired evaluation of the buccal and lingual bone plates.<sup>34</sup> Nonetheless, the use of CT may be linked to inaccuracies in detecting bone levels due to beam hardening metal artifacts.<sup>35</sup>

### ***Future directions***

Recent experimental findings suggested that implant surface characteristics influence the progression of peri-implantitis.<sup>31, 36</sup> In fact, a histological analysis revealed that the vertical dimensions of the lesion, the pocket epithelium and the apical extension of the biofilm were larger for micro-rough surfaces than for turned surfaces.<sup>31</sup> In the bargain, clinical<sup>37</sup> and preclinical<sup>38</sup> data pointed out that peri-implantitis resolution in implants with turned surface was more efficient than with micro-rough surfaces. Notwithstanding, to our best knowledge, this is the first experimental report testing the concept of hybrid implants compared to previous trials that evaluated machined-surface implants.<sup>1, 30, 31, 39</sup> Our findings indicated that implant surface characteristics in the coronal aspect of the influences the pro-inflammatory profile (IL-1 $\beta$ ) during spontaneous progression of peri-implantitis. From this data, it can be speculated that in individuals prone to develop peri-implantitis based on altered susceptibility (i.e., with history of periodontal disease, irregular supportive care or suboptimal plaque control),<sup>40</sup> or more pathogenic bacterial profile H implants with a machined collar under the platform could offer benefits in terms of reduced inflammatory profile for the prevention and arrestment of peri-implantitis. In fact, preclinical findings by Monje et al. (2018) in an experimental peri-implantitis model indicated that R implants presented with slightly greater MBL compared to H implants.<sup>12</sup>

### **Conclusion**

An increase in pathogenic bacteria is associated with ligature-induced progressive bone loss, bleeding and suppuration as consequence of experimental peri-implantitis. The spontaneous progression of the disease, however, is generally associated to a decrease in bacterial counts in the short-term. While *Pg* and *Tf* are associated with ligature-induced disease progression, *Pi* augments its load during the spontaneous progressive phase. Moreover, IL-1 $\beta$  is associated with pocket probing depth and is influenced by the implant surface characteristics during the spontaneous progression phase.

## Acknowledgement

The authors thank TICARE Implants (Valladolid, Spain) for funding of the study and the analyses. In addition, the FEDICOM foundation partially funded the study by providing surgical instruments, supplying accommodation, covering travel expenses for the principal investigator (Dr. Alberto Monje) and the laboratory analyses. We likewise thank Francisco Javier Vela (Centro de Cirugía Mínimamente Invasiva Jesús Usón, Cáceres, Spain) for his professionalism and kindness in housing the dogs.

## References

1. Charalampakis G, Abrahamsson I, Carcuac O, Dahlen G, Berglundh T. Microbiota in experimental periodontitis and peri-implantitis in dogs. *Clin Oral Implants Res* 2014;25:1094-1098.
2. Furst MM, Salvi GE, Lang NP, Persson GR. Bacterial colonization immediately after installation on oral titanium implants. *Clin Oral Implants Res* 2007;18:501-508.
3. Lafaurie GI, Sabogal MA, Castillo DM, et al. Microbiome and Microbial Biofilm Profiles of Peri-Implantitis: A Systematic Review. *J Periodontol* 2017;88:1066-1089.
4. Kumar PS, Mason MR, Brooker MR, O'Brien K. Pyrosequencing reveals unique microbial signatures associated with healthy and failing dental implants. *J Clin Periodontol* 2012;39:425-433.
5. Sanz-Martin I, Doolittle-Hall J, Teles RP, et al. Exploring the microbiome of healthy and diseased peri-implant sites using Illumina sequencing. *J Clin Periodontol* 2017;44:1274-1284.

6. Carcuac O, Berglundh T. Composition of human peri-implantitis and periodontitis lesions. *J Dent Res* 2014;93:1083-1088.
7. Galindo-Moreno P, Lopez-Martinez J, Caba-Molina M, et al. Morphological and immunophenotypical differences between chronic periodontitis and peri-implantitis - a cross-sectional study. *Eur J Oral Implantol* 2017;10:453-463.
8. Rakic M, Monje A, Radovanovic S, Petkovic-Curcin A, Vojvodic D, Tatic Z. Is the personalized approach the key to improve clinical diagnosis of peri-implant conditions? The role of bone markers. *J Periodontol* 2019.
9. Ramseier CA, Eick S, Bronnimann C, Buser D, Bragger U, Salvi GE. Host-derived biomarkers at teeth and implants in partially edentulous patients. A 10-year retrospective study. *Clin Oral Implants Res* 2016;27:211-217.
10. Ataoglu H, Alptekin NO, Haliloglu S, et al. Interleukin-1beta, tumor necrosis factor-alpha levels and neutrophil elastase activity in peri-implant crevicular fluid. *Clin Oral Implants Res* 2002;13:470-476.
11. Kilkenny C, Browne W, Cuthill IC, Emerson M, Altman DG, Group NCRGW. Animal research: reporting in vivo experiments: the ARRIVE guidelines. *The journal of gene medicine* 2010;12:561-563.
12. Monje A, Insua A, Rakic M, Nart J, Moyano-Cuevas JL, Wang HL. Estimation of the diagnostic accuracy of clinical parameters for monitoring peri-implantitis progression: An experimental canine study. *J Periodontol* 2018;89:1442-1451.
13. Grischke J, Karch A, Wenzlaff A, Foitzik MM, Stiesch M, Eberhard J. Keratinized mucosa width is associated with severity of peri-implant mucositis. A cross-sectional study. *Clin Oral Implants Res* 2019;30:457-465.
14. Mombelli A, van Oosten MA, Schurch E, Jr., Land NP. The microbiota associated with successful or failing osseointegrated titanium implants. *Oral Microbiol Immunol* 1987;2:145-151.

15. Monje A, Insua A, Monje F, et al. Diagnostic accuracy of the implant stability quotient in monitoring progressive peri-implant bone loss: An experimental study in dogs. *Clin Oral Implants Res* 2018;29:1016-1024.
16. Sanguansermsri P, Nobbs AH, Jenkinson HF, Surarit R. Interspecies dynamics among bacteria associated with canine periodontal disease. *Mol Oral Microbiol* 2018;33:59-67.
17. Maruyama N, Mori A, Shono S, Oda H, Sako T. Evaluation of changes in periodontal bacteria in healthy dogs over 6 months using quantitative real-time PCR. *Pol J Vet Sci* 2018;21:127-132.
18. Eke PI, Braswell LD, Fritz ME. Microbiota associated with experimental peri-implantitis and periodontitis in adult *Macaca mulatta* monkeys. *J Periodontol* 1998;69:190-194.
19. Tillmanns HW, Hermann JS, Tiffée JC, Burgess AV, Meffert RM. Evaluation of three different dental implants in ligature-induced peri-implantitis in the beagle dog. Part II. Histology and microbiology. *Int J Oral Maxillofac Implants* 1998;13:59-68.
20. Nociti FH, Jr., Cesco De Toledo R, Machado MA, Stefani CM, Line SR, Goncalves RB. Clinical and microbiological evaluation of ligature-induced peri-implantitis and periodontitis in dogs. *Clin Oral Implants Res* 2001;12:295-300.
21. Zhu B, Meng H, Huang B, Chen Z, Lu R. Detection of *T. forsythia* and other important bacteria in crestal and subcrestal implants with ligature-induced peri-implant infection in dogs. *J Periodontol* 2019;90:306-313.
22. Linares A, Pico A, Blanco C, Blanco J. Adjunctive Systemic Metronidazole to Nonsurgical Therapy of Peri-implantitis with Intra-bony Defects: A Retrospective Case Series Study. *Int J Oral Maxillofac Implants* 2019;34:1237-1245.
23. Nart J, Pons R, Valles C, Esmatges A, Sanz-Martin I, Monje A. Non-surgical therapeutic outcomes of peri-implantitis: 12-month results. *Clin Oral Investig* 2020;24:675-682.

24. Heitz-Mayfield LJA, Salvi GE, Mombelli A, Faddy M, Lang NP. Anti-infective surgical therapy of peri-implantitis. A 12-month prospective clinical study. *Clin Oral Implants Res* 2012;23:205-210.
25. Garaicoa-Pazmino C, Fretwurst T, Squarize CH, et al. Characterization of macrophage polarization in periodontal disease. *J Clin Periodontol* 2019;46:830-839.
26. Renvert S, Widen C, Persson GR. Cytokine expression in peri-implant crevicular fluid in relation to bacterial presence. *J Clin Periodontol* 2015;42:697-702.
27. Schierano G, Pejrone G, Brusco P, et al. TNF-alpha TGF-beta2 and IL-1beta levels in gingival and peri-implant crevicular fluid before and after de novo plaque accumulation. *J Clin Periodontol* 2008;35:532-538.
28. Kany S, Vollrath JT, Reija B. Cytokines in Inflammatory Disease. *Int J Mol Sci* 2019;20.
29. Schwarz F, Herten M, Sager M, Bieling K, Sculean A, Becker J. Comparison of naturally occurring and ligature-induced peri-implantitis bone defects in humans and dogs. *Clin Oral Implants Res* 2007;18:161-170.
30. Carcuac O, Abrahamsson I, Albouy JP, Linder E, Larsson L, Berglundh T. Experimental periodontitis and peri-implantitis in dogs. *Clin Oral Implants Res* 2013;24:363-371.
31. Albouy JP, Abrahamsson I, Berglundh T. Spontaneous progression of experimental peri-implantitis at implants with different surface characteristics: an experimental study in dogs. *J Clin Periodontol* 2012;39:182-187.
32. Dabdoub SM, Tsigarida AA, Kumar PS. Patient-specific analysis of periodontal and peri-implant microbiomes. *J Dent Res* 2013;92:168S-175S.
33. Isidor F. Clinical probing and radiographic assessment in relation to the histologic bone level at oral implants in monkeys. *Clin Oral Implants Res* 1997;8:255-264.

34. Ritter L, Elger MC, Rothamel D, et al. Accuracy of peri-implant bone evaluation using cone beam CT, digital intra-oral radiographs and histology. *Dentomaxillofac Radiol* 2014;43:20130088.
35. Benic GI, Sancho-Puchades M, Jung RE, Deyhle H, Hammerle CH. In vitro assessment of artifacts induced by titanium dental implants in cone beam computed tomography. *Clin Oral Implants Res* 2013;24:378-383.
36. Fickl S, Kebschull M, Calvo-Guirado JL, Hurzeler M, Zuhr O. Experimental Peri-Implantitis around Different Types of Implants - A Clinical and Radiographic Study in Dogs. *Clin Implant Dent Relat Res* 2015;17 Suppl 2:e661-669.
37. Berglundh T, Wennstrom JL, Lindhe J. Long-term outcome of surgical treatment of peri-implantitis. A 2-11-year retrospective study. *Clin Oral Implants Res* 2018;29:404-410.
38. Almohandes A, Carcuac O, Abrahamsson I, Lund H, Berglundh T. Re-osseointegration following reconstructive surgical therapy of experimental peri-implantitis. A pre-clinical in vivo study. *Clin Oral Implants Res* 2019;30:447-456.
39. Carcuac O, Abrahamsson I, Derks J, Petzold M, Berglundh T. Spontaneous progression of experimental peri-implantitis in augmented and pristine bone: A pre-clinical in vivo study. *Clin Oral Implants Res* 2020;31:192-200.
40. Dreyer H, Grischke J, Tiede C, et al. Epidemiology and risk factors of peri-implantitis: A systematic review. *J Periodontal Res* 2018;53:657-681.



## Figure legends

**Figure 1.** Implant designs tested in the present study (left: micro-roughened implant surface – R; right: hybrid design with machined surface at the coronal portion – H)

**Figure 2.** Marginal bone loss (mm) along the study period. MB: mesio-buccal; DB: disto-buccal; ML: mesio-lingual; DL: disto-lingual

**Figure 3.** Graphs showing the bacterial counts along the study period. Note: x-axis indicate timepoints; y-axis: mean±standard deviation. (a) summary of bacterial counts, (b) total bacterial counts (16S), (c) *Porphyromonas gulae* (Pg), (d) *Tannerella forsythia* (Tf), (e) *Neisseria canis* (Nc), (f) *Prevotella intermedia* (Pi), (g) *Fusobacterium nucleatum* (Fn), (h) *Parvimonas micra* (Pm), (i) *Campylobacter rectus* (Cr), (j) interleukin IL-1 $\beta$ .

**Figure 4.** Statistically significant correlations reached between (a) 16S and marginal bone loss (MBL measured in mm), (b) modified sulcular bleeding index (y-axis: score) and total bacterial counts (16S), (c) IL-1 $\beta$  and probing pocket depth (PPD measured in mm)

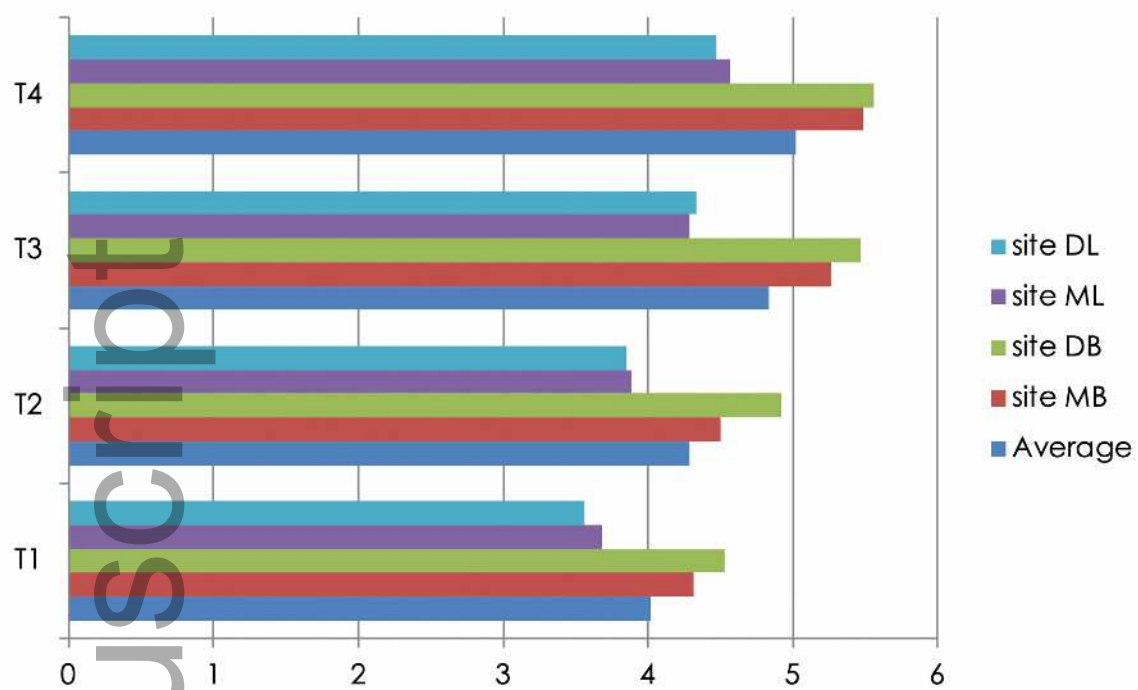
**Figure 5.** IL-1 $\beta$  along the study period for hybrid (H) and rough (R) implants

**Supplementary table 1.** Per time point and global correlations between the clinical and radiographic parameters and bacteria and host-related biomarkers analyzed.

Author Manuscript



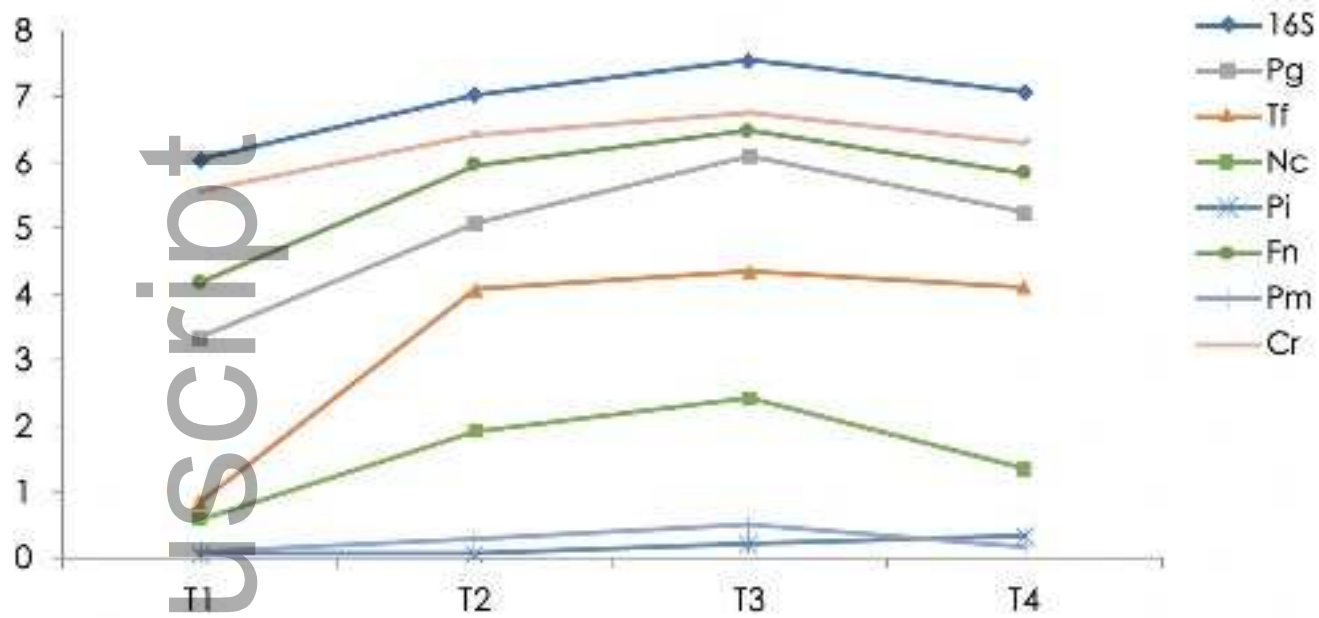
jre\_12797\_f1.png



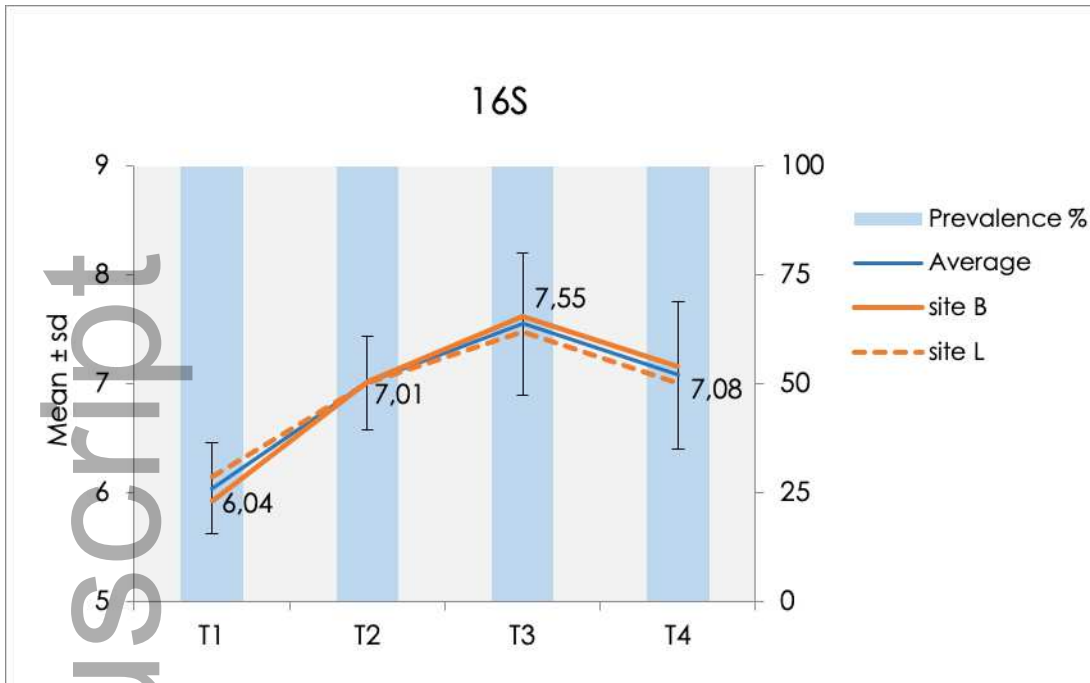
jre\_12797\_f2.png

Author Manuscript

Author Manuscript



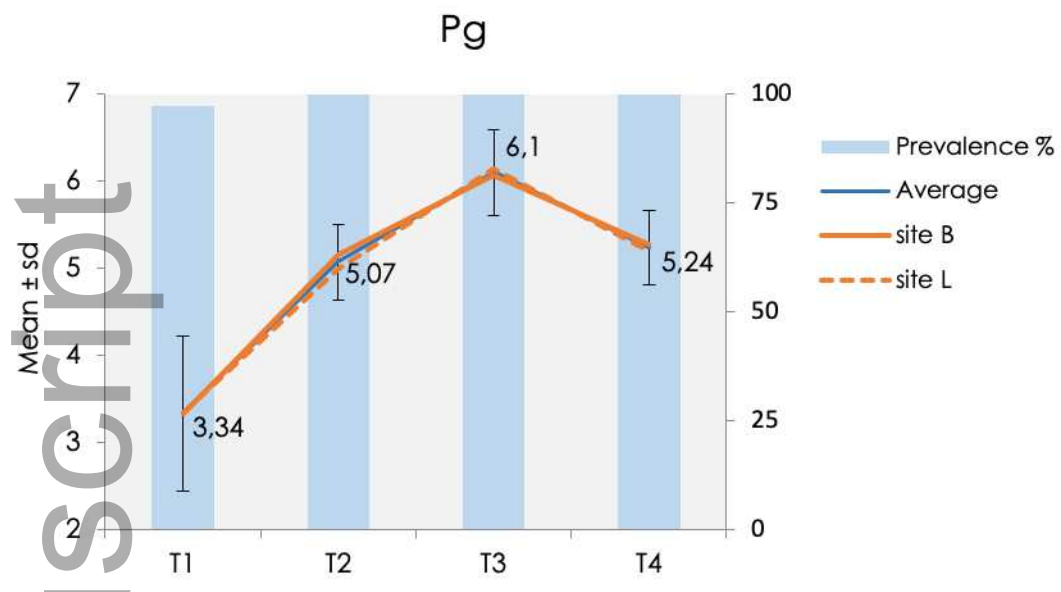
jre\_12797\_f3a.tiff



jre\_12797\_f3b.png

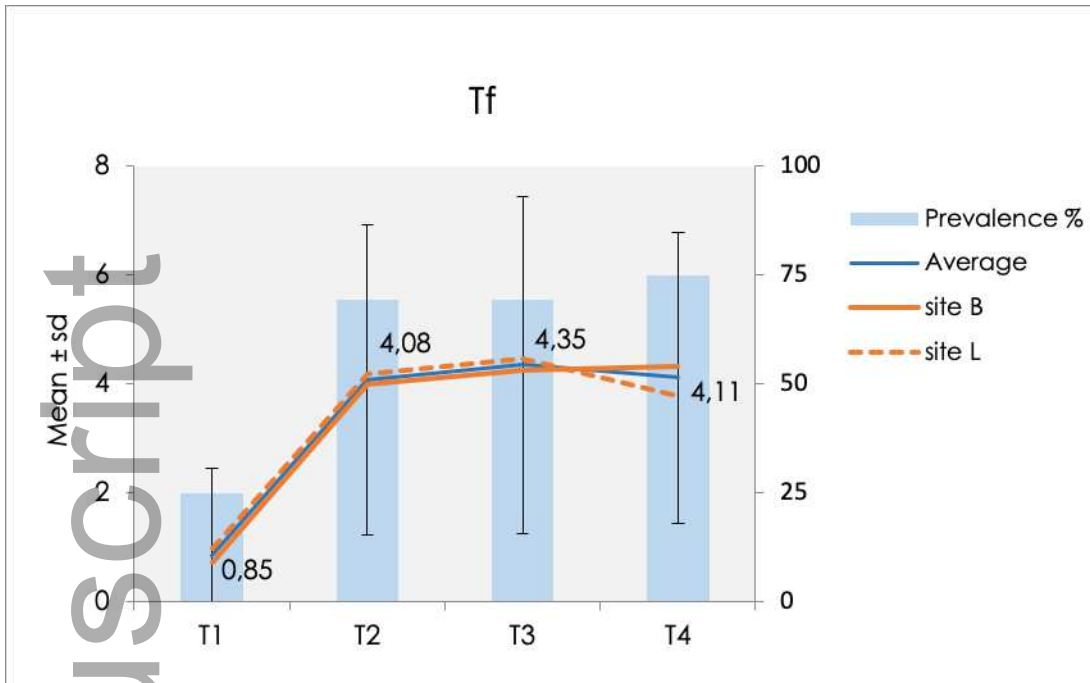
Author Manuscript

Author Manuscript

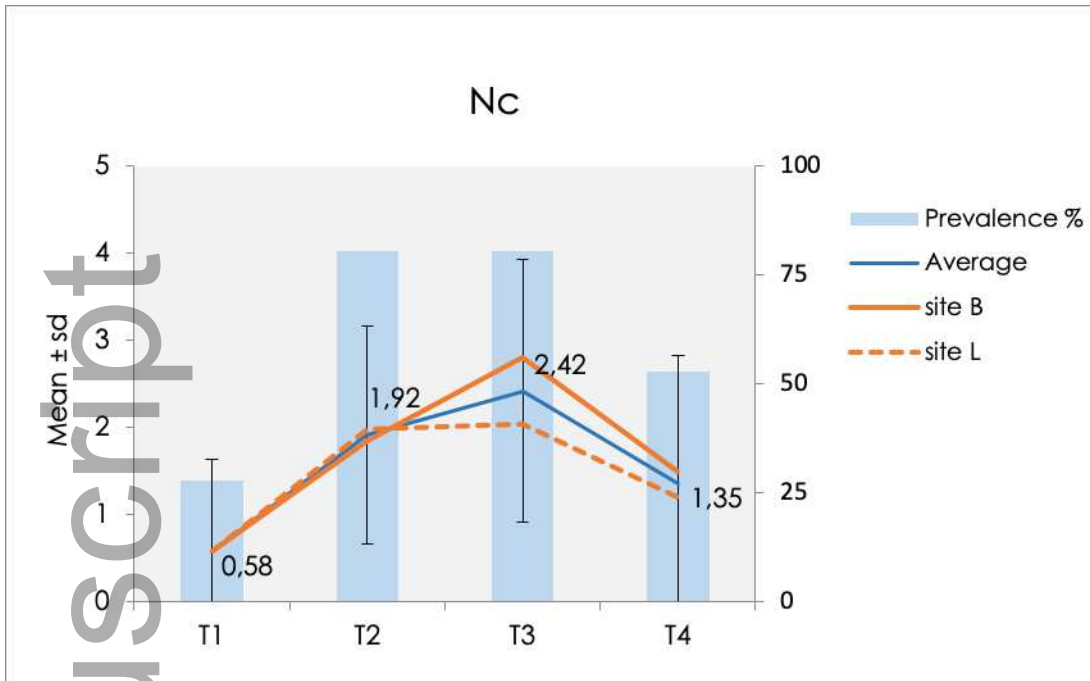


jre\_12797\_f3c.png

Author Manuscript

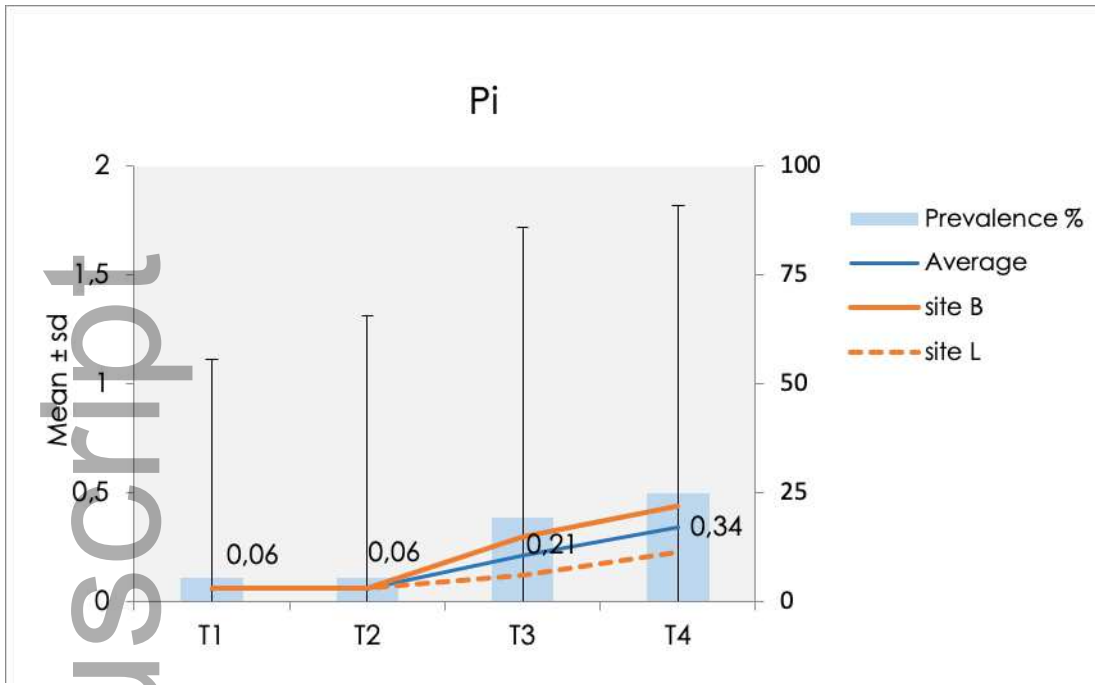


jre\_12797\_f3d.png



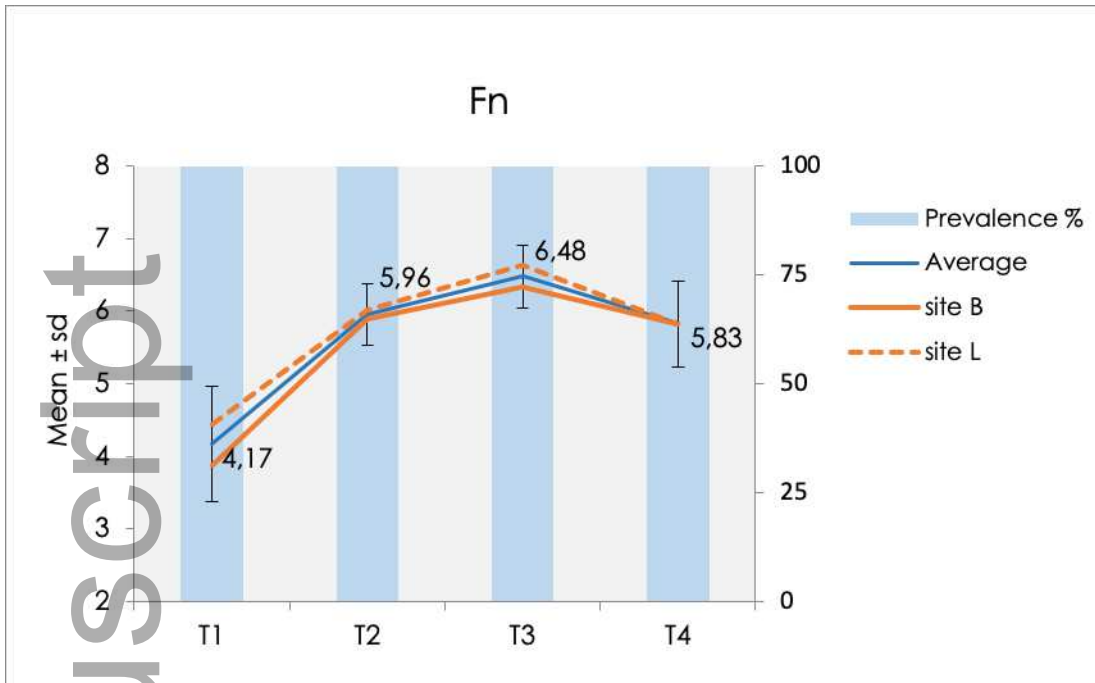
jre\_12797\_f3e.png





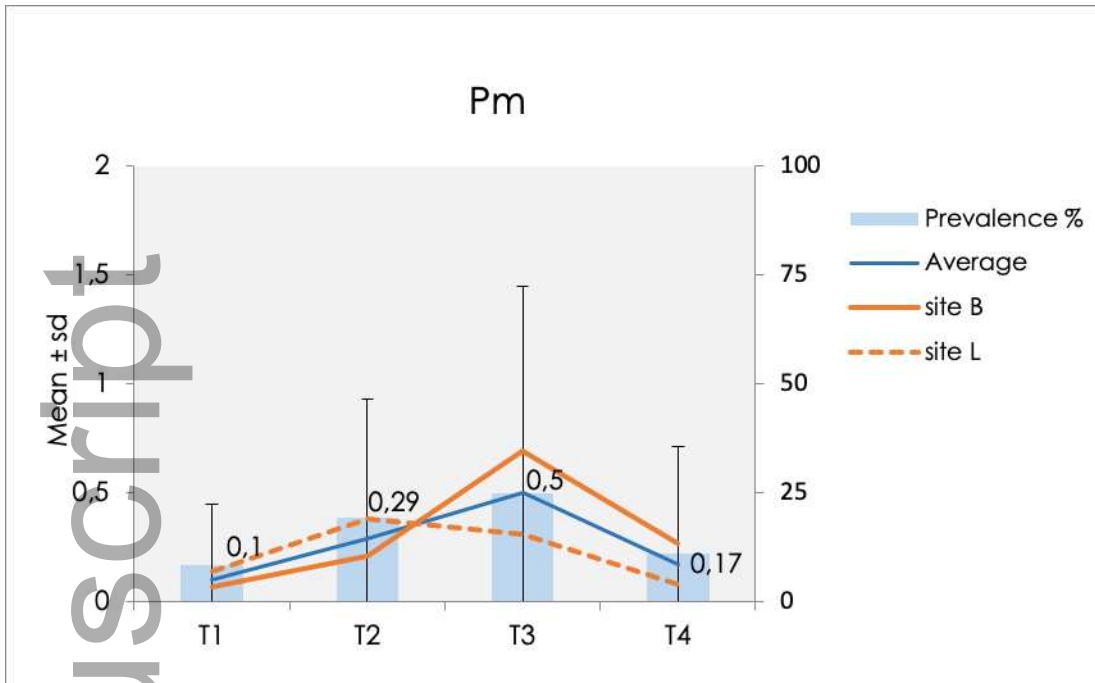
jre\_12797\_f3f.png

Author Manuscript



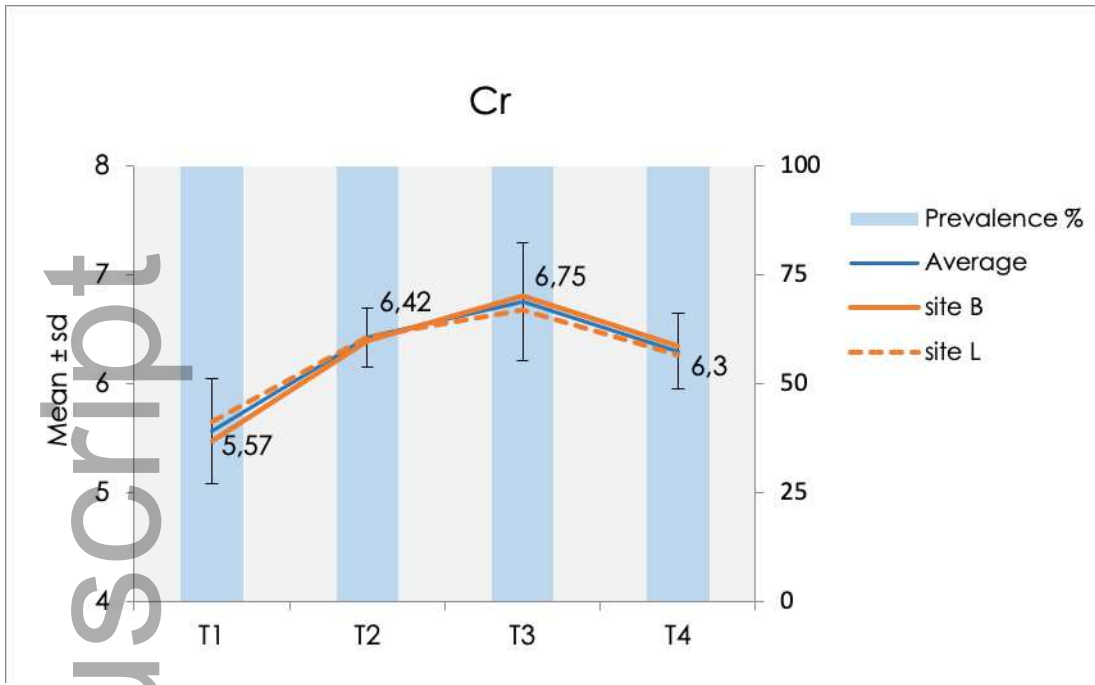
jre\_12797\_f3g.png

Author Manuscript



jre\_12797\_f3h.png

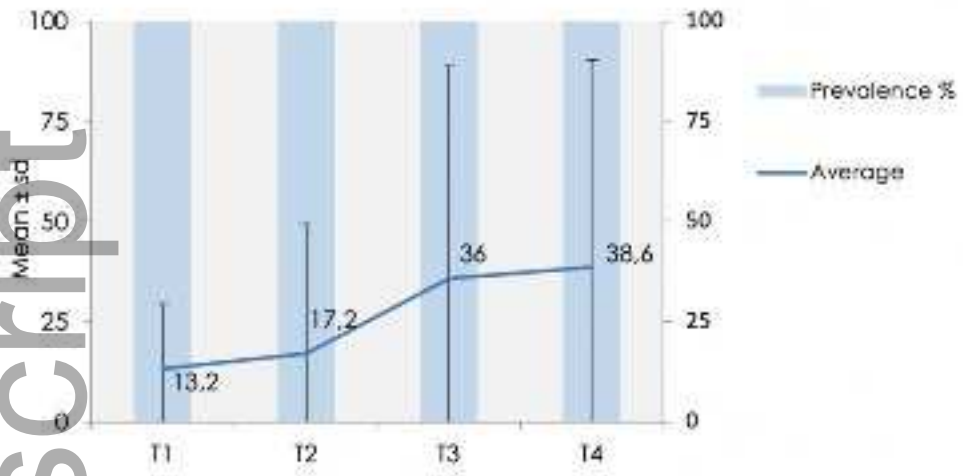
Author Manuscript



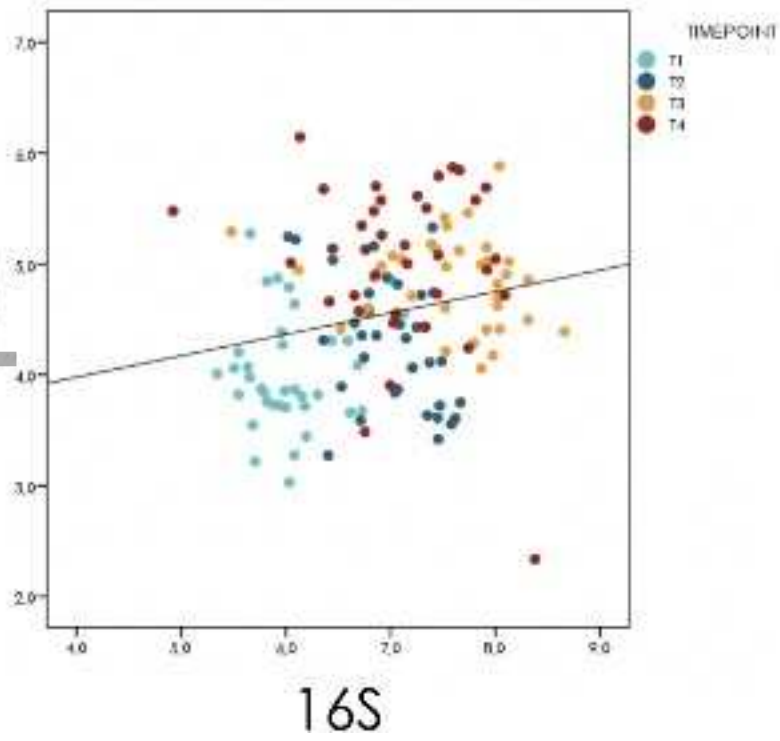
jre\_12797\_f3i.png

Author Manuscript

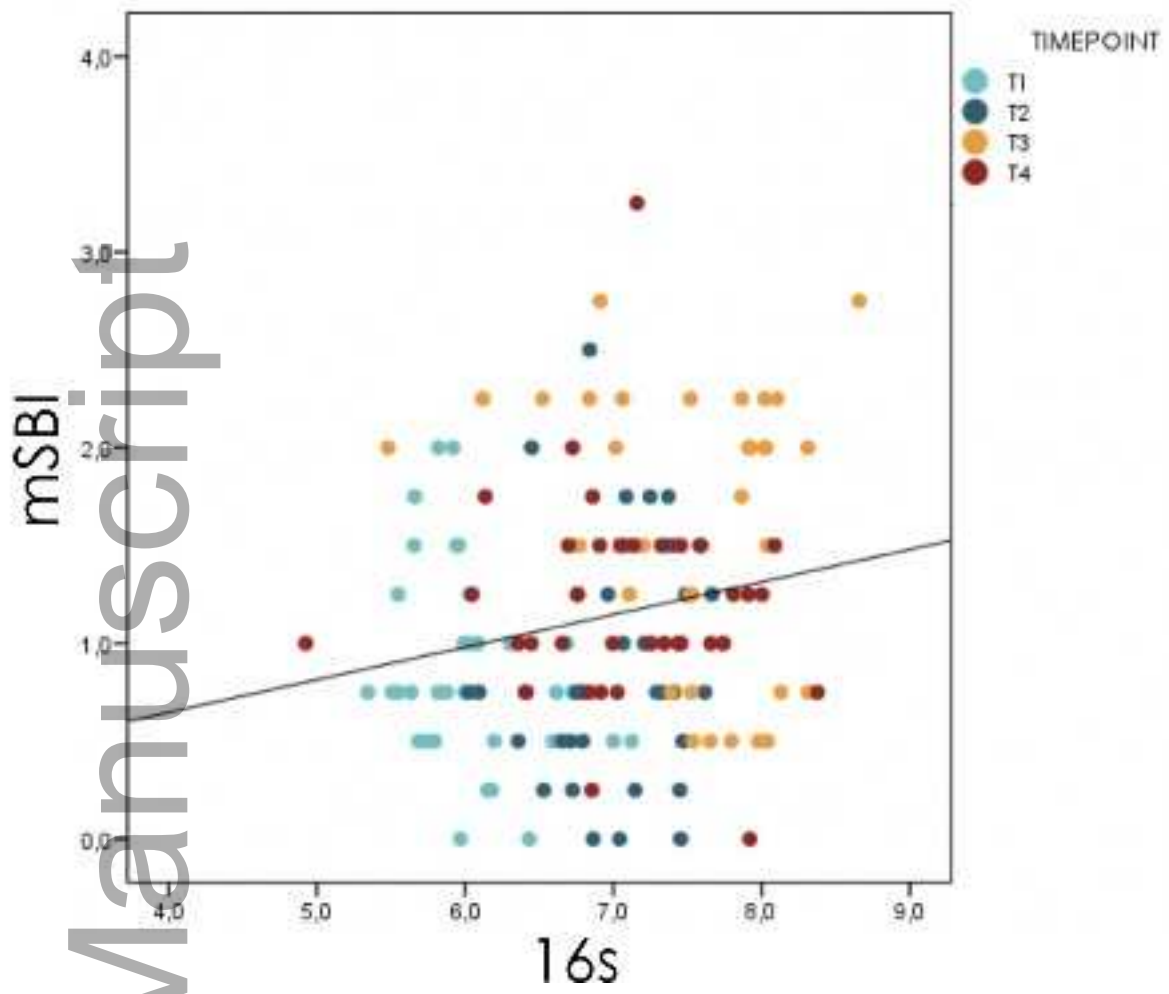
### IL-1 $\beta$



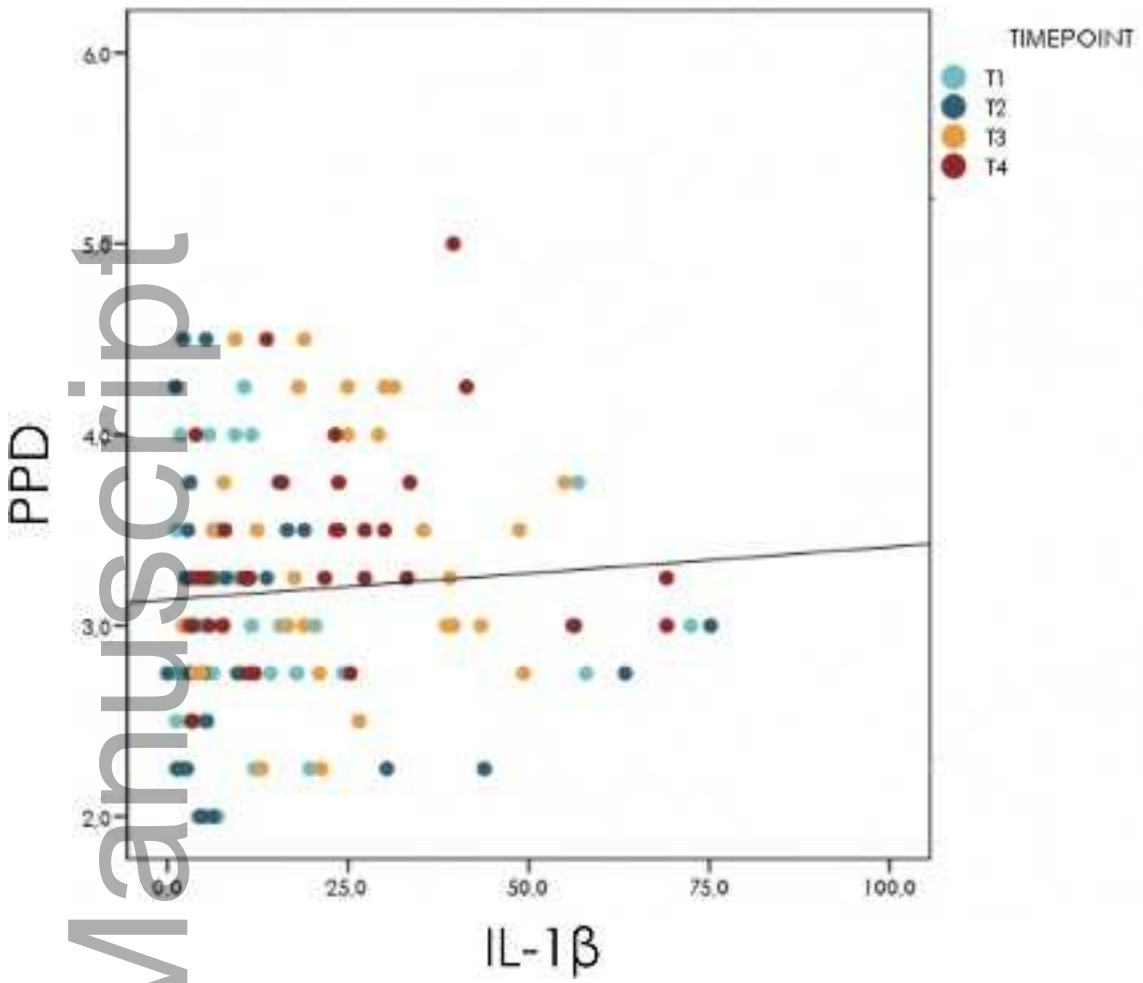
jre\_12797\_f3j.png



16S  
jre\_12797\_f4a.png

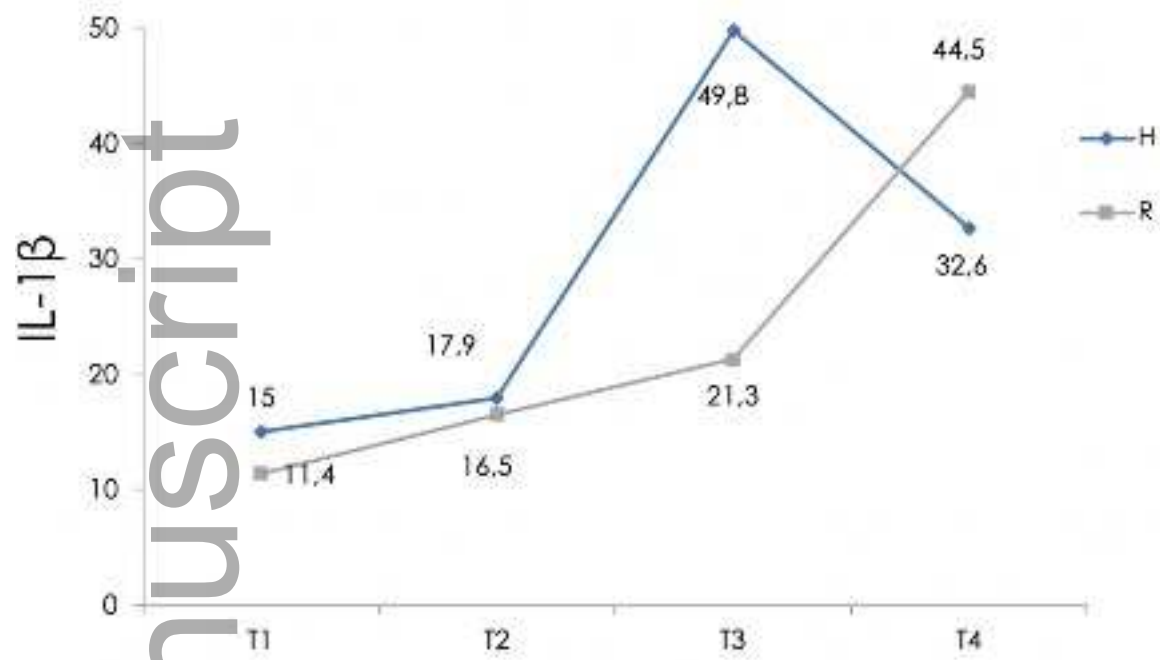


jre\_12797\_f4b.png



jre\_12797\_f4c.png





jre\_12797\_f5.tiff